Supplementary information

Figure S1 IR-induced dose-dependent changes of the phosphorylation of FLAG-H2AX in the stable cells. (**A**) 293T cells stably expressing FLAG-tagged H2AX (FLAG-H2AX cells) were irradiated at the indicated dose, lysed (1h after the radiation), and the lysates were analyzed by immunoblotting (IB). IB was done first with anti-FLAG antibody and then the same PVDF membrane was re-probed with anti-γH2AX antibody. The bands near 26 kDa indicated FLAG-tagged H2AX which presented at a constant level and served as the loading control. The level of phosphorylated FLAG-H2AX increased in an IR dose-dependent manner. (**B**) MS spectra of AACT-containing peptides of the representative proteins identified in the IP mixture. Peptide sequences are, NDLAVVDVR (Nucleolin), KELAAQLNEEAKR (Spt16), ILQDSLGGR (KIF11), MSVQPTVSLGGFEITPPVVLR (NPM1), LDQQTLPLGGR (RBM10) and TTNFAGILSQGLR (PARP1). The IR-induced dose-dependent binding to H2AX was quantified based on the isotope ratio of particular arginine-containing peptides. (**C**) Immunoblot validation of these dose-dependent H2AX interactions identified based on quantitative MS data. The FLAG-H2AX immunoprecipitates isolated from either non-radiated or irradiated cells were subjected to immunoblotting with the indicated antibodies. As a loading control the amount of H2AX was measured by blotting against anti-FLAG antibodies. (* indicates the signals cross-reactive with light chain immunoglobulin). Lane 1 to 3, Input; lane 4 to 6, empty vector-purified control; lane 7, 9 and 11, mock-purified control; lane 8, 10 and 12, dose-dependent H2AX-associating proteins.

Figure S2 Domain analysis of H2AX interactome identified by MS-based quantitative proteomics. (**A**) A two-dimensional hierarchical clustering map was constructed by TreeView programming where individual modular domains were arrayed in the vertical axis, and

individual proteins found to contain the closely related sets of modular domains were clustered in a phylogenic manner along the horizontal axis. Four prominent clusters are indicated by green, white, yellow, and blue boxes. The 'zoom-in' clusters are shown in (**B**), (**C**), (**D**), and (**E**), with the protein/domain identities (see Experimental Procedures for details). All proteins shown in Fig. S2 and Table S3 were identified by using the criteria described in the Experimental Procedures (*Mass spectrometry*) and quantified based on the Experimental Procedures (*AACT-based quantitation for distinguishing dose-dependent H2AX interactors*). A total of 69 proteins were identified with high confidence. Among them, 18 proteins showed the IR-induced changes in their interactions with H2AX. In the hierarchal clustering map, we identified four prominent clusters in the green, yellow, white and blue box respectively (Fig. S2). As shown in Fig. S2*B* (green box), a common feature of these proteins is that all contains WD40 domain, which linked the neighboring phylogenic trees to a variety of the functions ranging from signal transduction, transcription regulation, cell cycle control, to protein modification. Also some of our identified H2AX-interacting proteins were found containing characteristic domains such as chromo (SMRC1), PHD (JHDM3A and BPTF), Tudor (JHDM3A), bromo (BPTF), WD40 (BUB3, RACK1, MEP50, EIF3I and GNB2L1), and BRCT (PARP1) which are known to involve in the regulations of chromatin structure, post-translational modification on histones, cell cycle checkpoint functions response to DNA damage and apoptosis. Through identification of their containing of Ku, SAP and DNA Toposo IV domains which are known as the DNA/RNA binding domains, those proteins in yellow and white clusters (Fig. S2*C* and *D*) are grouped in the function associating with DNA repair and rejoining of DNA ends. The proteins in the blue cluster all containing contractile domains such as AAA and RRM domain (Fig. S2*E*) were found to link with diverse functions. For example, RBM10, HNRNPA1, EIF4B, and PABP1 are involved in the regulatory processes of mRNA metabolism whereas NUBP1, Nucleolin, and HNRNPCL1 play critical

roles in nucleosome assembly. This hierarchical clustering allowed for a systematic categorization of H2AX-interacting proteins into the corresponding function subsets and then identified those linked biological processes.

Figure S3 The functional networks in the IR inducible H2AX interactome. The IR-inducible H2AX interaction network was mapped based on our identified γH2AX interactors by using STRING, which contains both known and predicted protein-protein interactions indicative of those physical (direct) and functional (indirect) associations. The dose-dependent associations with H2AX (Table S2) were indicated by colors with proteins in pink box being those more associated with H2AX at both dose levels of 7.5 cGy and 10 Gy. The low dose (7.5 cGy)-sensitive associations are in lime green box and the high dose (10 Gy)-sensitive associations are in red box. The proteins in light blue box dissociate from H2AX upon radiation at both dose levels, and low dose-sensitive dissociations are in brown box. The proteins not identified by MS but found in known database are in gray box. Purple lines indicate those interactions identified by experiments, and light green lines suggest possible connectivity through data mining.

Figure S4 The knock-down of BCLAF1 suppressed p53 expression. 293T cells were transfected with mock (lane 1), *BCLAF1* siRNA (40 nM; lane 2) or scrambled siRNA (40 nM; lane 3) respectively and then left for 2 days. Cell lysates were subjected to immunoblotting analysis with anti-BCLAF1 (upper panel), anti-p53 (middle panel) or anti-GAPDH (bottom panel).

Figure S5 Effect of BCLAF1 knock-down on the growth and morphology of differentially irradiated A549 cells in higher magnification format. DAPI was used to stain DNA.

Figure S6 Product ion spectrum of a phosphopeptide (SSSSRSSSPYSK) derived from MS/MS-collision-induced dissociation (CID) found in the BCLAF1 isolated from 10 Gy-irradiated *DNA-PKcs*$^{+/-}$ (top panel) and *DNA-PKcs*$^{-/-}$ (bottom panel) MEF cells. The upper inset in the top panel is an expanded view of product ions between *m/z* 520-660, and the lower one shows all major b- and y-type product ions assigned to the peptide sequence on the basis of dominant backbone fragment ions. Both Ser-151and Tyr-150 were identified as phosphorylated sites.

Figure S7 Label-free quantitation based on MS1 peak area of the phosphopeptide precursor ions of (SSSSRSSSPYSK) found in the BCLAF1 isolated from 10 Gy-irradiated *DNA-PKcs*$^{-/-}$ (top panel) and *DNA-PKcs*$^{+/-}$ (bottom panel) MEF cells. Note that the peak represents an isobaric mixture of phosphopeptides comprising phosphorylations at S151 and Y150. Total spectral counts of all the proteins found in each sample were used to normalize the total BCLAF1protein levels found in both *DNA-PKcs*$^{-/-}$ and *DNA-PKcs*$^{+/-}$ MEF cells. The normalized spectral counts for BCLAF1 showed a ratio of 1 between *DNA-PKcs*$^{-/-}$ and *DNA-PKcs*$^{+/-}$. In addition, the basal phosphorylation levels of BCLAF1 peptide SSSSRSSSPYSK in both *DNA-PKcs*$^{-/-}$ and *DNA-PKcs*$^{+/-}$ implicates phosphorylation at Y150 in BCLAF1 in addition to its phosphorylation at S151. The phosphorylation at Y150 has been reported (1) in BCLAF1 and our data suggests that its occupancy is independent of DNA-PKcs.

Figure S8 Product ion spectrum corresponding to high energy collision dissociation (HCD) of doubly protonated SSSSRSSSPYSK-phosphopeptide sequence found in BCLAF1. The two possible phosphorylation sites are highlighted based on phosphospecific cleavages. Note that m/z *216 Da* corresponds to phosphtyrosine immonium ions and is shown as **Im(pY)** and

another phosphoserine immonium ion is indicated as **Im(pS)**. This spectrum verified the possibility of an isobaric mixture of phosphopeptides comprising both S151 and Y150 phosphorylation. The corresponding phosphoimmonium reporter ions for both pS-151 and pY-150 supports that the wild-type *DNA-PKcs*$^{+/-}$ cells comprise phosphorylation at both sites in concordance with our label-free phosphopeptide quantitation results.

Reference

1. Linding, R., Jensen, L. J., Ostheimer, G. J., van Vugt, M. A., Jørgensen, C., Miron, I. M., Diella, F., Colwill, K., Taylor, L., Elder, K., Metalnikov, P., Nguyen, V., Pasculescu, A., Jin, J., Park, J. G., Samson, L. D., Woodgett, J. R., Russell, Robert B., Bork, P., Yaffe, M. B., and Pawson, T. (2007) *Cell* **129**, 1415-1426

Supplement Fig. 1

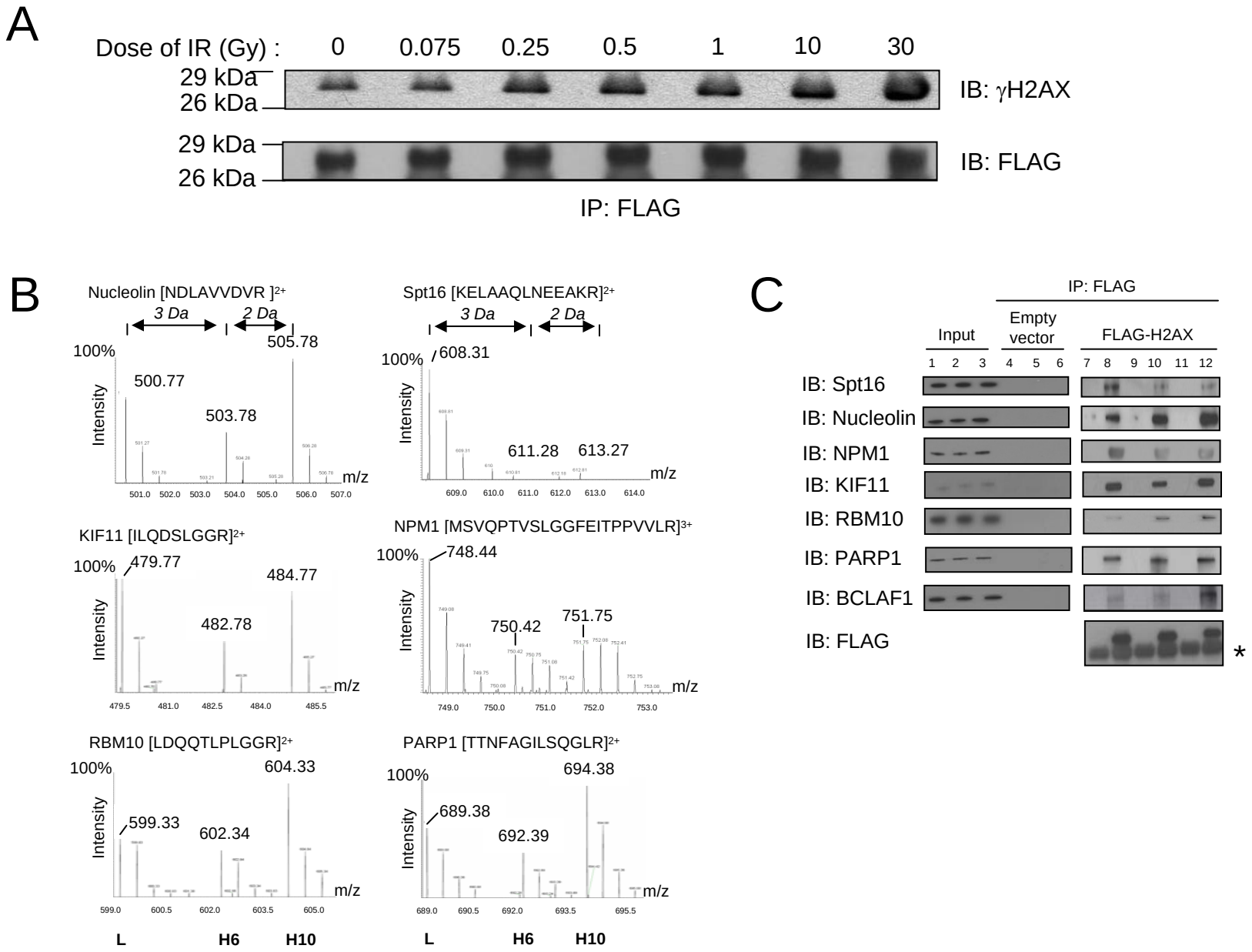

Supplement Fig. 2

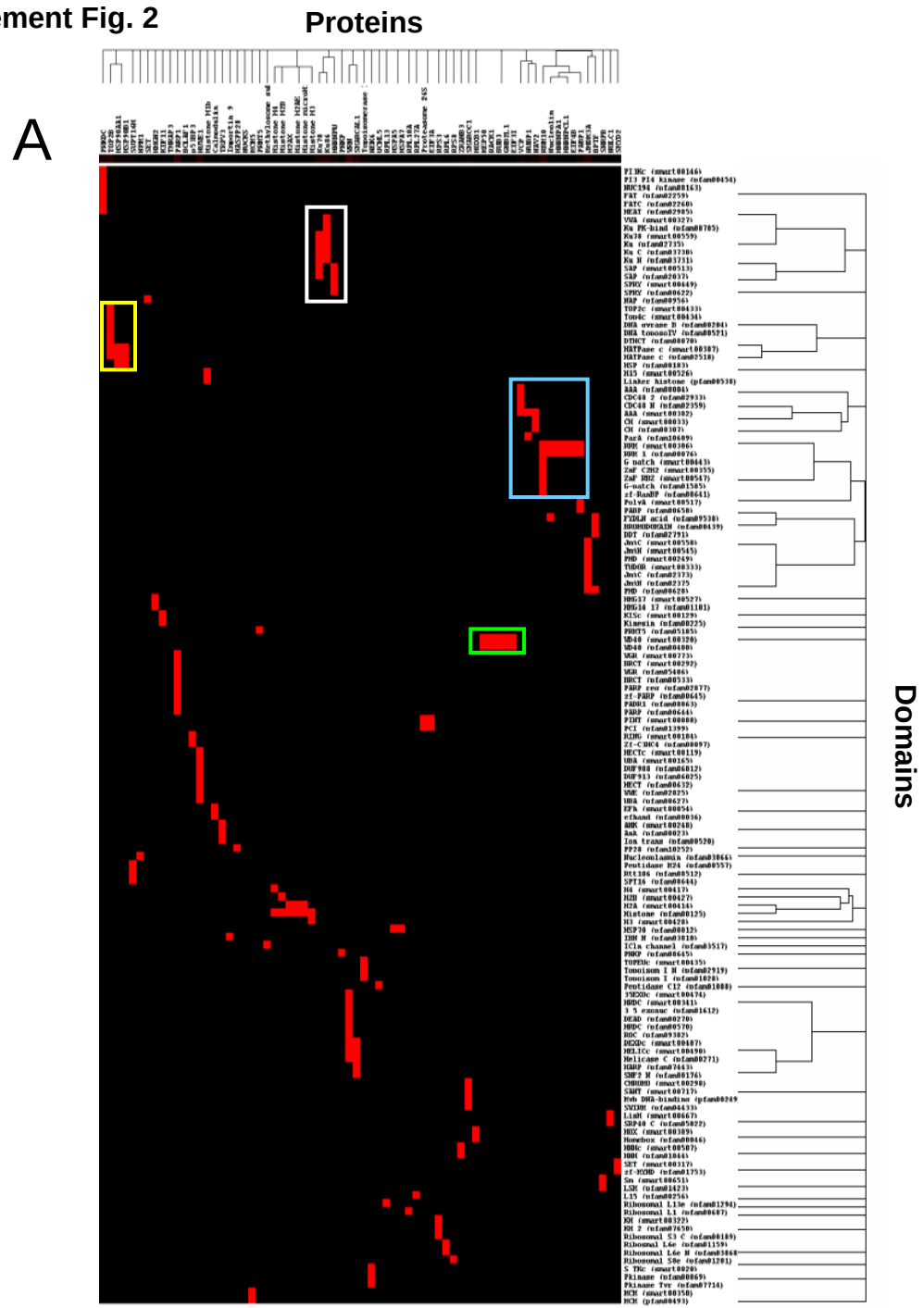

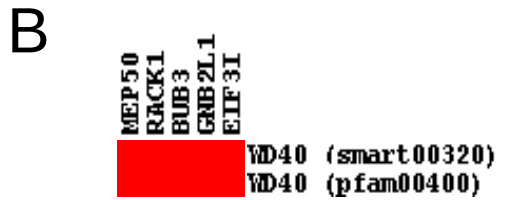

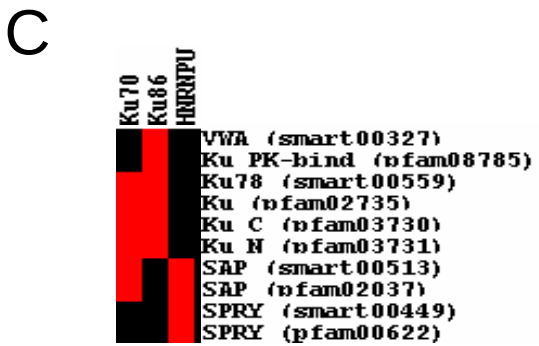

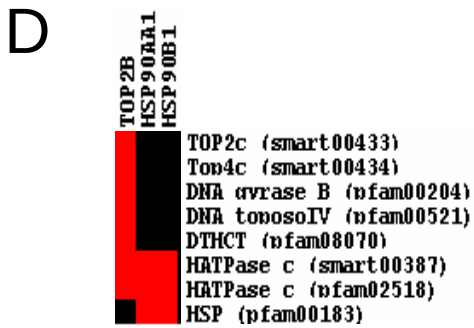

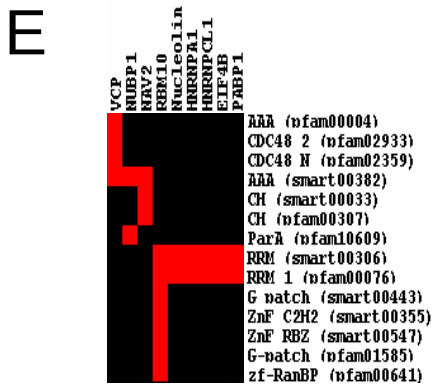

Supplement Fig. 3

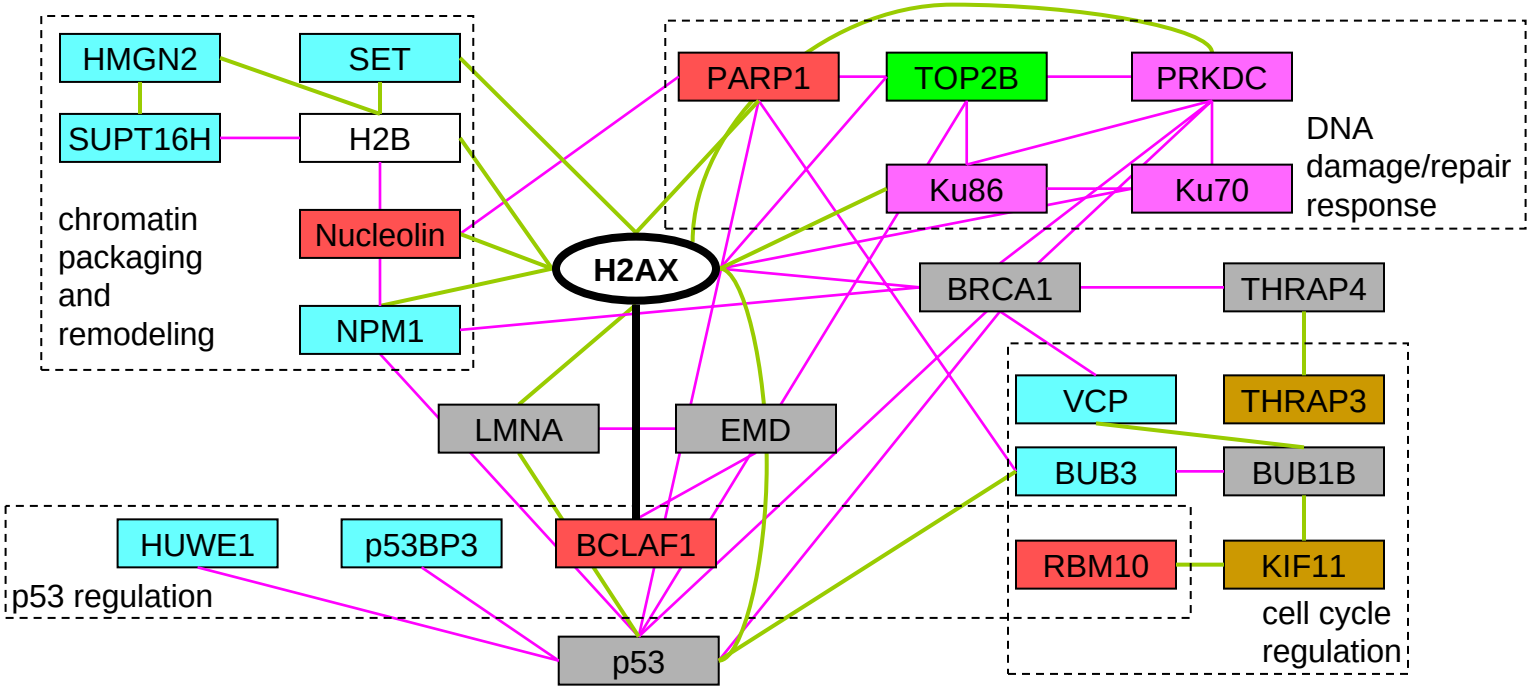

Supplement Fig. 4

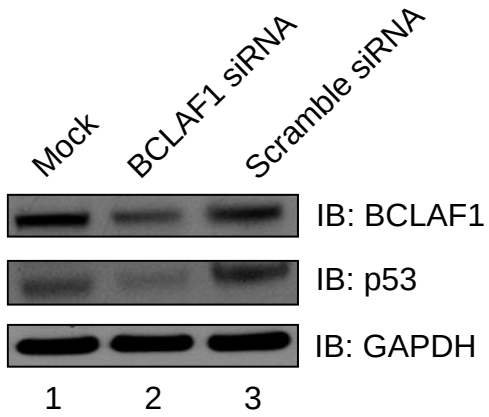

Supplement Fig. 5

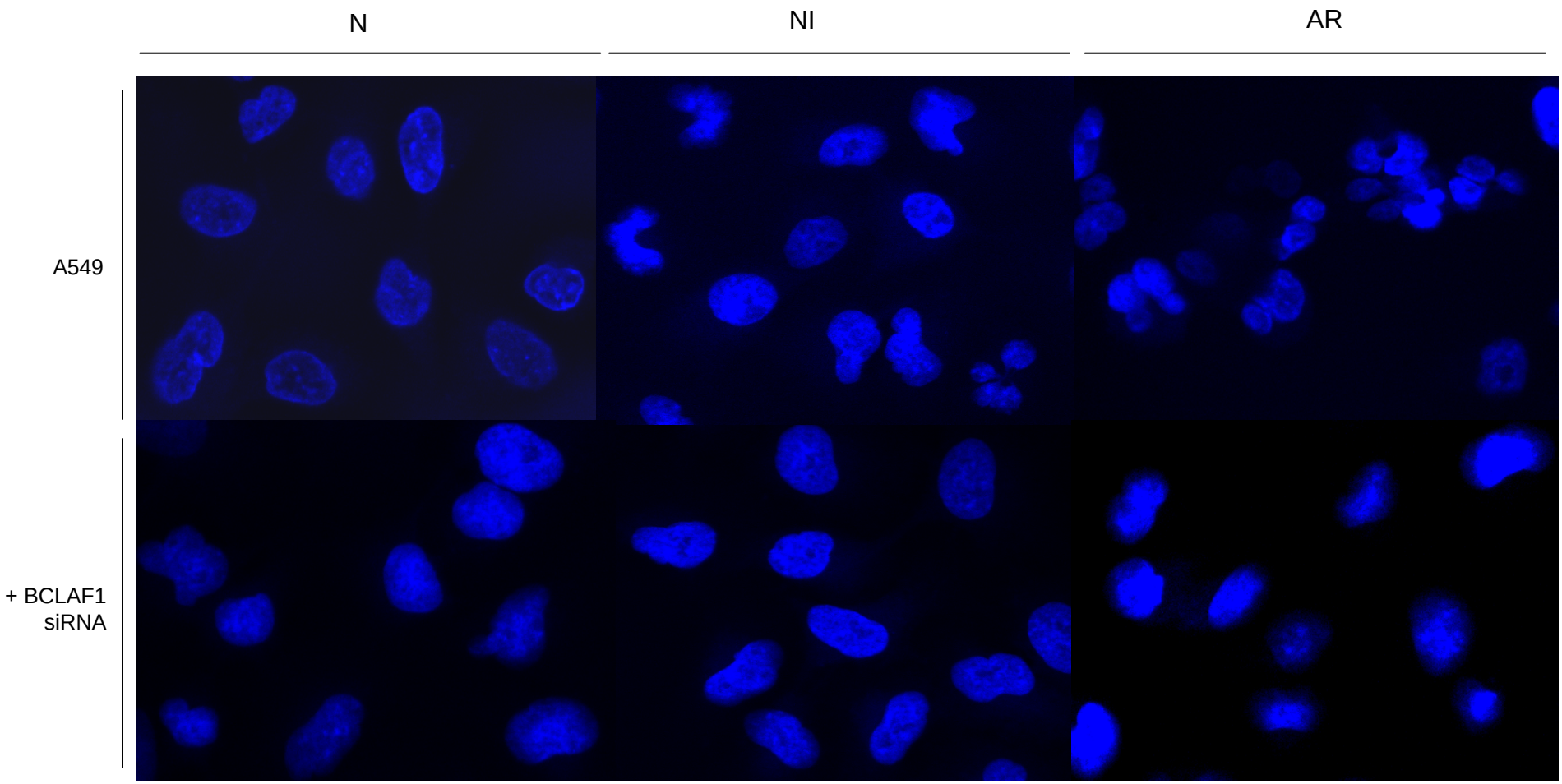

Supplement Fig. 6

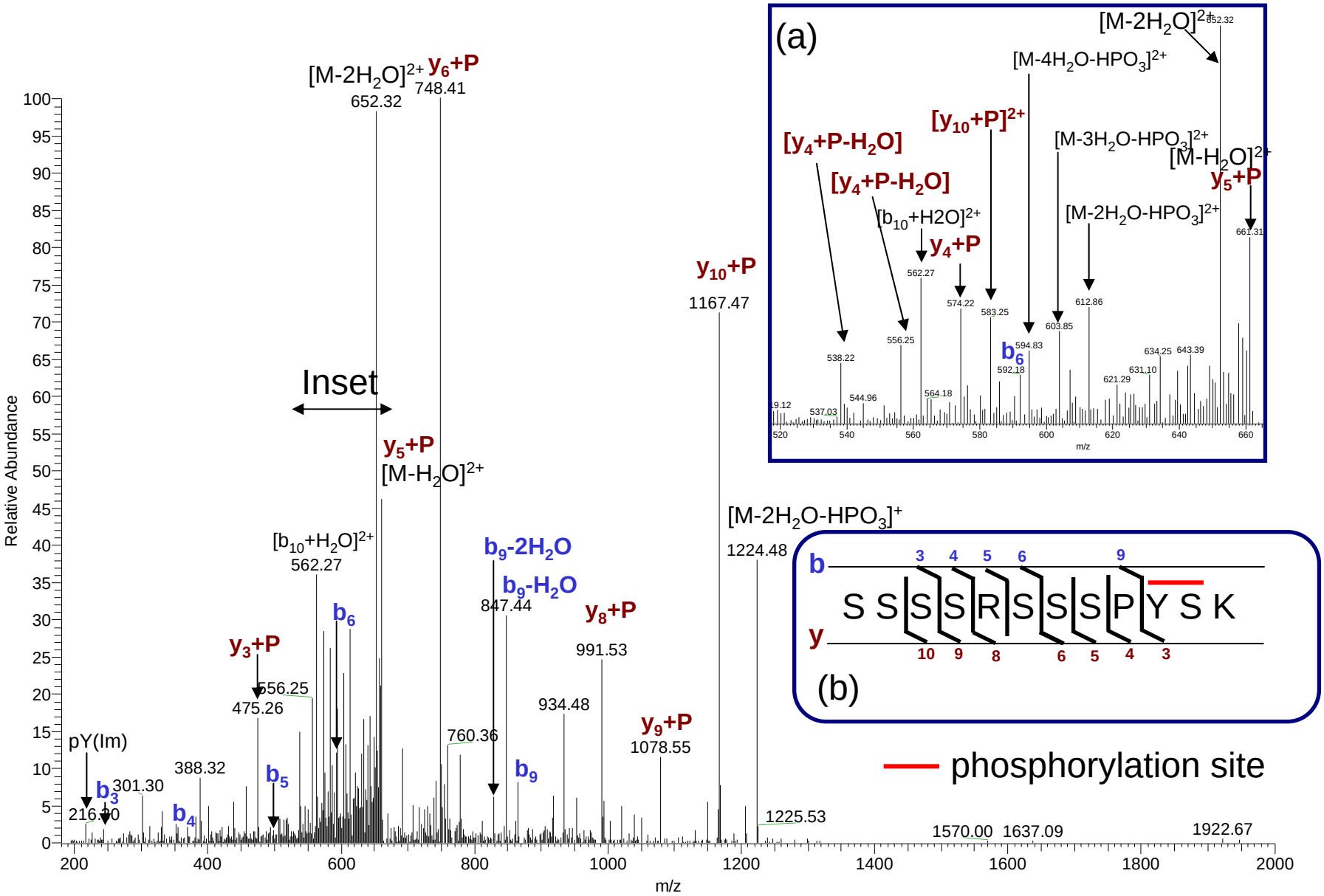

Supplement Fig. 7

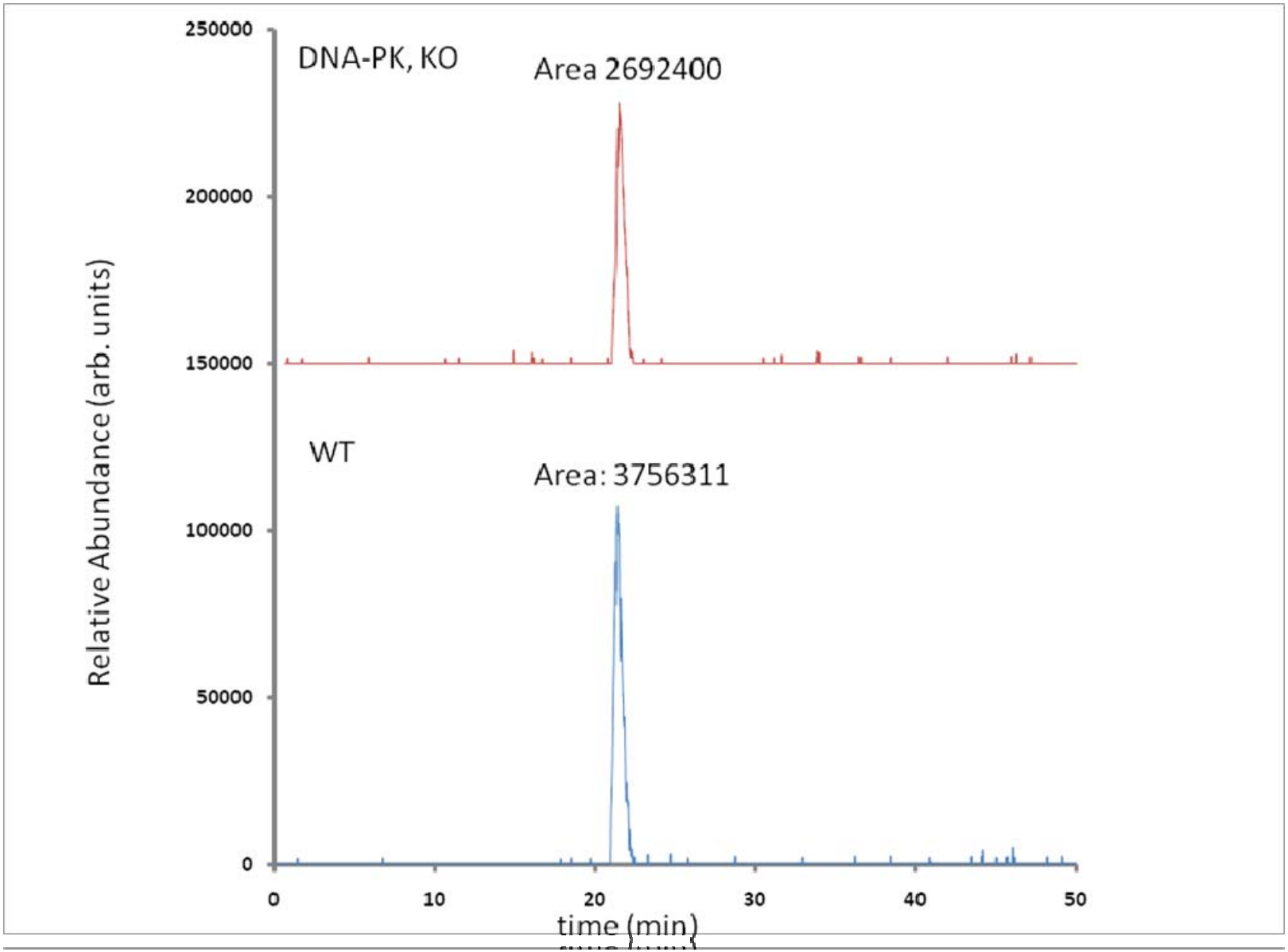

Supplement Fig. 8

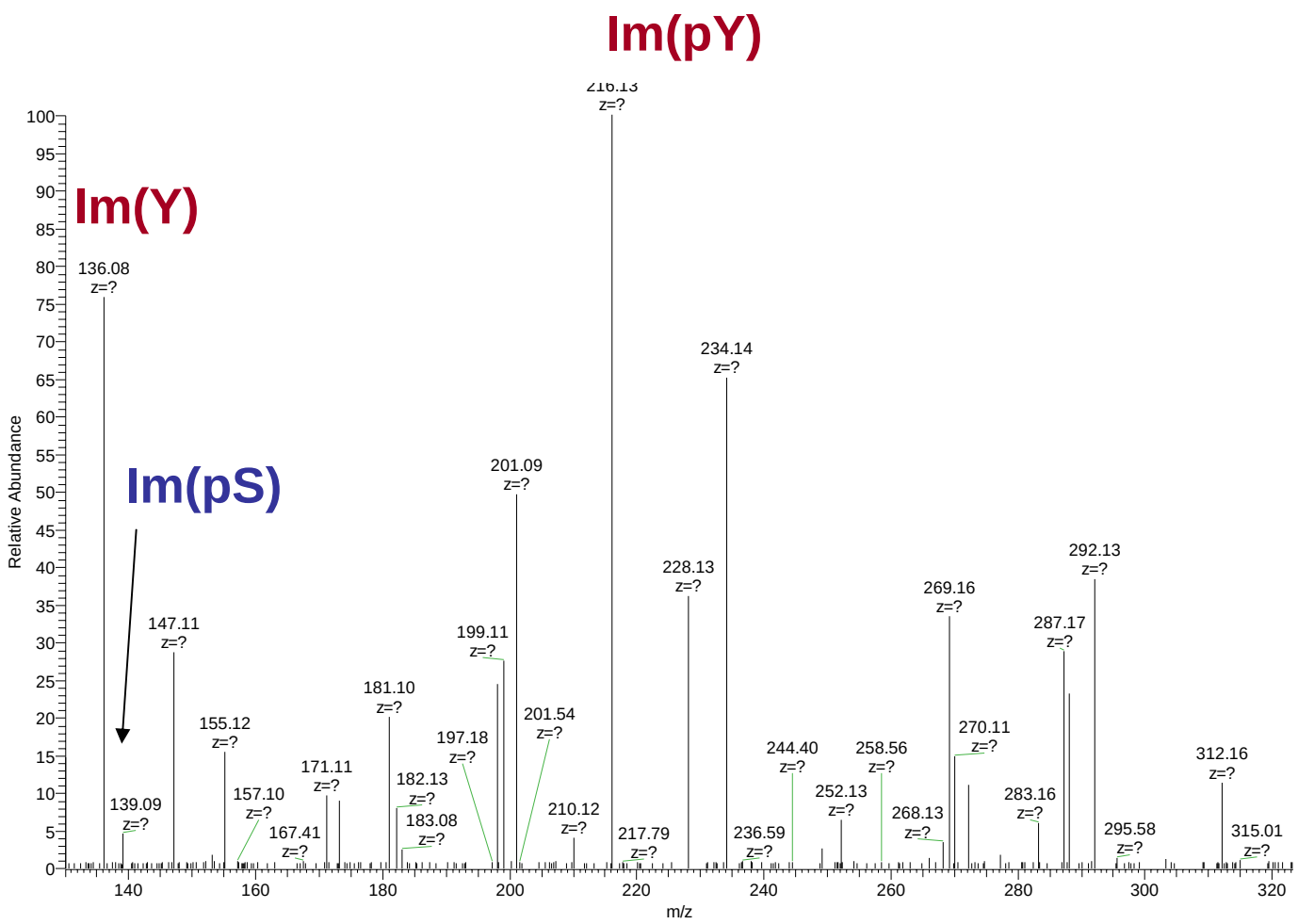

Supplemental Table 1. The Peptides Derived From the Immunoprecipitates Identified by MS					
NCBI accession no.	Protein Name	Peptide Identified	Ion Score[a]	Protein Score[b]	Peptide Score[c]
1. Histones					
gi|48146275	Histone H2AX (bait)	GHYAER HLQLAIR KGHYAER AGLQFPVGR LLGGVTIAQGGVLPNIQAVLLPK AGLQFPVGR	41 44 31 65 17 -	198	- - - - - 2.54
gi|356168	Histone H1b	SGVSLAALKK ALAAAGYDVEK ASGPPVSELITK KASGPPVSELITK ALAAAGYDVEKNNSR SGVSLAALKK ALAAAGYDVEK ASGPPVSELITK	30 37 65 79 87 - - -	298	- - - - - 2.73 3.58 3.11
gi|10800144	Histone H2A, member E	GNYAER KGNYAER AGLQFPVGR VTIAQGGVLPNIQAVLLPK	22 41 73 106	242	-
gi|1568557	Histone H2B	EIQTAVR LAHYNKR LLLPGELAK	40 37 30	107	-
gi|1568559	Histone H3	IRGERA KLPFQR YRPGTVALR	31 22 15	68	-
gi|45767731	Histone H4	TLYGFGG	43	303	-

		VFLENVIR ISGLIYEETR DNIQGITKPAIR ISGLIYEETRGVLK KTVTAMDVVYALKR DNIQGITKPAIRR	21 38 112 17 21 51		
gi|3493529	Histone microH2A1.2	SIAFPSIGSGR	21	21	-
2. Intracellular protein traffic and signaling cascade					
a. Ca^{2+} binding/signaling					
gi|825671	Nucleophosmin/B23 (NPM1)	ADKDYHFK VDNDENEHQLSLR MTDQEAIQDLWQWR FINYVK MSVQPTVSLGGFEITPPVVLR	34 96 18 - -	148	- - - 2.24 4.85
gi|825635	Calmodulin (CALM1)	VFDKDGNGYISAAELR	68	68	-
gi|21435923	Transient receptor potential cation channel subfamily V member 3 (TRPV3)	RMYDMILLR	40	40	-
b. Protein import					
gi|21361659	Importin 9 (IPO9)	LLQHGINADDKR EALVDTLTGILSPVQEVR	18 17	35	-
3. Signal transduction					
gi|2498464	28 kDa heat- and acid-stable phosphoprotein (HASPP28)	MQSLSLNK VTQLDLDGPK GVEGLIDIENPNR	- - -	-	2.56 2.99 3.66
gi|15559817	Guanine nucleotide-binding protein subunit beta-2-like 1 (GNB2L1)	DETNYGIPQR DVLSVAFSSDNR	47 18	65	-
gi|47605556	Bcl-2-associated transcription factor 1 (BCLAF1/Btf)	IDISPSTLR EYSGFAGVSR SSFYPDGGDQETAK VFLLDR	 - -		- - 3.31 2.22

gi|31874030	RNA-binding protein 10 (RBM10)	GSSYGVTSTESYK LDQQTLPLGGR TINVEFAK ESATADAGYAILEK	- - - -	-	3.14 3.03 2.29 4.11
gi|97537467	Thyroid hormone receptor-associated protein 3 (THRAP3)	TDSEKPFR SPLQSVVVR YKDDPVDLR SIFQHIQSAQSQR ASAVSELSPR GSFSDTGLGDGK SPLQSVVVR.R	18 31 34 16 - - -	99	- - - - 3.22 3.43 2.57
4. Cell cycle					
gi|11095436	Transitional endoplasmic reticulum ATPase (VCP)	HPALFK GDIFLVR	32 18	50	-
gi|1155084	Kinesin-like protein KIF11 (KIF11)	QIDVYR TPHVPYR NGVYISEENFR LNLVDLAGSENIGR ILQDSLGGR IGAVEEELNR LLNTVEETTK VTELFMDNK LTDNGTEFSVK ETTIDGEELVK LNLVDLAGSENIGR	19 13 18 51 - - - - - - -	101	- - - - 2.47 3.68 3.23 2.73 2.93 2.84 3.23
gi|7387554	Mitotic checkpoint protein BUB3 (BUB3)	KLNQPPEDGISSVKF RVAVEYLDPSPEVQKK	- -	-	2.94 3.82
gi|10437591	Nuclear ubiquitous casein and cyclin-dependent kinases substrate (NUCKS)	SSPREAKNK	29	29	-
gi|13177775	Minichromosome maintenance deficient protein	RYRVGTDR	27	27	

	5 (MCM5)				
5. Protein metabolism and modification					
gi|2323410	Protein arginine N-methyltransferase 5 (PRMT5)	LYNEVR SDLLLSGR EFIQEPAK VPLVAPEDLR YSQYQQAIYK AAILPTSIFLTNK LSPWIRPDSK DDGVSIPGEYTSFLAPISSSK	30 24 30 61 50 34 32 21	282	-
gi|14495615	Methylosome protein 50 (WDR77)	ILLWDTR ETPPPLVPPAAR SDGALLLGASSLSGR VWDLAQQVVLSSYR KETPPPLVPPAAR ILLWDTR YRSDGALLLGASSLSGR SDGALLLGASSLSGR YEHDDIVSTVSVLSSGTQAVSGSK VWDLAQQVVLSSYR	36 46 37 17 - - - - - -	136	- - - - 3.24 2.60 4.11 4.97 4.28 5.06
gi|8571386	Methylosome subunit pICln (CLNS1A)	SFPPPGPAEGLLR	31	31	-
gi|157502195	Proteasome 26S non-ATPase regulatory subunit 1 (PSMD1)	VLDLQQIK LNIGDLQVTK	- -	-	2.80 3.11
gi|833318444	Heat shock protein HSP 90-alpha (HSP90AA1)	ALLFVPR APFDLFENR RAPFDLFENR HFSVEGQLEFR GVVDSEDLPLNISR ADHGEPIGR IDIIPNPQER	37 15 18 18 28 19 35	170	-

gi|119360	Endoplasmin (HSP90B1)	KSGTSEFLNKM RSGYLLPDTKA KLIINSLYKN KSILFVPTSAPRG	- - - -	-	2.61 2.74 2.86 3.60
gi|86577744	78 kDa glucose-regulated protein (HSPA5)	KITITNDQNRL KVLEDSDLKK RTWNDPSVQQDIKF KDAGTIAGLNVMRI KNQLTSNPENTVFDAKR KSQIFSTASDNQPTVTIKV RITPSYVAFTPEGERL RNELESYAYSLKN KELEEIVQPIISKL KTFAPEEISAMVLTKM	- - - - - - - - - -	-	2.84 2.31 3.38 3.79 4.51 5.14 4.11 3.40 4.21 3.82
gi|158518381	Putative heat shock 70 kDa protein 7 (HSPA7)	RVEILANDQGNRT	-	-	3.85
gi|55859546	Ubiquitin carboxyl-terminal hydrolase isozyme L5 (UCHL5)	KEFSQSFDAAMKG RLDTIFFAKQ	- -	-	2.74 2.31
gi|10121890	Serine/threonine-protein kinase Nek6 (NEK6)	RLIPER	24	24	-
gi|40788326	Lysine-specific demethylase 4A (KDM4A)	VINSRYR GSAARSFSER	15 12	27	
gi|38174276	E3 ubiquitin-protein ligase Topors (TOPORS)	ETKHKR RSTSLSSPR	11 12	23	
gi|56417899	E3 ubiquitin-protein ligase HUWE1 (HUWE1)	ITPAMAARIK FDMAENVVIVASQKRPLGGR	24 24	48	
6. Nucleoside, nucleotide and nucleic acid metablolism					
a. DNA repair and damage					
gi|22902366	Poly (ADP-ribose) polymerase 1 (PARP1)	KPPLLNNADSVQAK VVSEDFLQDVSASTK IAPPEAPVTGYMFGK LLWHGSR	110 110 52 22	596	- - - -

		AEPVEVVAPR	41		-
		TLGDFAAEYAK	59		-
		SKLPKPVQDLIK	19		-
		TTNFAGILSQGLR	29		-
		HPDVEVDGFSELR	36		-
		HASHISK	27		-
		YWIFR	8		-
		EWVTPK	19		-
		WDDQQK	15		-
		EELGFRPEYSASQLK	19		-
		AEPVEVVAPR	30		-
		DSEEAEIIR	-		2.98
		AEPVEVVAPR	-		2.82
		PVQDLIK	-		2.73
		GGSDDSSKDPIDVNYEK	-		4.29
		QQVPSGESAILDR	-		2.70
		GIYFADMVSK	-		3.14
		GFSLLATEDK	-		3.56
		TLGDFAAEYAK	-		3.83
		VVSEDFLQDVSASTK	-		5.37
		TTNFAGILSQGLR	-		4.38
		VFSATLGLVDIVK	-		4.17
gi|13606056	DNA-dependent protein kinase catalytic subunit (PRKDC)	TFPVLLR	12	84	-
		LLEEALLR	20		
		SIGEYDVLR	13		
		LGNPIVPLNIR	24		
		LGASLAFNNIYR	15		
gi|49457432	ATP-dependent DNA helicase 2 subunit 1 (Ku70)	ILELDQFK	31	83	-
		KPGGFDISLFYR	21		
		SDSFENPVLQQHFR	21		
gi|10863945	ATP-dependent DNA helicase 2 subunit 2	LGGHGPSFPLK	71	257	-

	(Ku86)	ANPQVGVAFPHIK FFMGNQVLK TLFPLIEAK YAYDKR FSEEQR FNNFLK SILQER KEEASGSSVTAEEAKK KVITMFVQRQ RYGSDIVPFSKV	68 27 30 14 10 16 21 - - -		- - - - - - - 4.34 2.78 3.57
gi|37231	DNA topoisomerase 2-beta (TOP2B)	FLYDDNQR EVTFVPGLYK ELILFSNSDNER SIPSLVDGFKPGQR	29 32 27 16	99	-
gi|5739524	Werner syndrome ATP-dependent helicase (WRN)	DISENLYSLR	20	20	
gi|5764101	Bifunctional polynucleotide phosphatase/kinase (PNKP)	MGEVEAPGR	17	17	
gi|20072751	DNA topoisomerase I (TOP1)	SRSVLEK LNXLDPR	21 20	41	
b. Chromatin packaging and remodeling					
gi|6005757	FACT complex subunit SPT16 (SUPT16H)	RVMEIVDADEKV KELAAQLNEEAKR KAASITSEVFNKF	- - -	-	2.72 3.55 3.39
gi|49457053	Protein SET (SET)	RVEVTEFEDIKS RLNEQASEEILKV RIDFYFDENPYFENKV	- - -	-	4.04 3.88 5.26
gi|89040736	Non-histone chromosomal protein HMG-17 (HMGN2)	VKDEPQRR LSAKPAPPKPEPK	30 62	92	- -
gi|13559170	Nucleotiide-binding protein 1 (NUBP1)	PGNLAGVR	20	20	-

gi|6693791	SWI/SNF-related matrix-associated actin-dependent regulator of chromatin subfamily A-like protein 1 (SMARCAL1)	IDGSTSSAER	20	20	-
gi|1549239	SWI/SNF complex subunit SMRCC1 (SMRCC1)	RFDLQNPSR	17	17	
gi|6683492	Nucleosome-remodeling factor subunit BPTF (BPTF)	DATPLSR	19	19	
c. Pre-mRNA processing					
gi|3183544	Polyadenylate-binding protein 1 (PABPC1)	SGVGNIFIK ALDTMNFDVIK	- -	-	2.31 3.27
gi|31455242	Nucleolin (NCL)	NDLAVVDVR ALELTGLK EVFEDAAEIR TGISDVFAK GIAYIEFK KGLSEDTTEETLKE RSISLYYTGEKG	- - - - - - -	-	3.29 2.33 2.87 2.73 2.44 3.32 3.32
gi|145559503	Nucleolar phosphoprotein p130 (NOLC1)	RDNQLSEVANKF KAALSLPAKQ	- -	-	3.11 2.30
gi|14141163	Heterogeneous nuclear ribonucleoprotein U (HNRNPU)	KNGQDLGVAFKI KYNILGTNTIMDKM	- -	-	2.65 4.18
gi|45709273	Heterogeneous nuclear ribonucleoprotein A1 (HNRNPA1)	KTFNPGAGLPTDKK KGLLQSGQIPGRE IEVIEIMTDR	- - -	-	2.68 3.68 3.65
gi|33877030	Heterogeneous nuclear ribonucleoprotein CL1 (HNRNPCL1)	KSDVEAIFSKY RVFIGNLNTLVVKK	- -	-	2.80 3.72
gi|134037	Small nuclear ribonucleoprotein-associated protein B and B' (SNRPB)	RGENLVSMTVEGPPPKD RVLGLVLLRG	- -	-	4.92 2.74
d. mRNA transcription regulation					
gi|64654265	Homeobox protein Hox-B1 (HOXB1)	RNPPKTGR	21	21	-

gi|217540605	Zinc finger Ran-binding domain-containing protein 3 (ZRANB3)	RYCNAHIR	21	21	-
gi|9910274	SET and MYND domain-containing 2 (SMYD2)	KEGLSKCGR	18	18	
e. Translation Processing					
gi|4503513	Eukaryotic translation initiation factor 3 subunit I (EIF3I)	RDMTMFVTASKD KSYSSGGEDGYVRI KSGEVLVNVKE RDPSQIDNNEPYMKI RQINDIQLSRD KLFDSTTLEHQKT REGDLLFTVAKD	- - - - - - -	-	3.57 4.01 3.56 4.24 2.39 3.40 2.91
gi|1399801	Eukaryotic translation inititation factor 3 subunit A (EIF3A)	RDEERPR	22	22	-
gi|50053795	Eukaryotic translation initiation factor 4B (EIF4B)	KVAPAQPSEEGPGRK RGLNISAVRL	- -	-	2.35 2.49
gi|4506625	60S ribosomal protein L27a (RPL27A)	AKFFSRR	20	20	-
gi|62204505	60S ribosomal protein L13 (RPL13)	KLATQLTGPVMPVRN RGFSLEELRV	- -	-	3.19 2.22
gi|4490422	60S ribosomal protein L10a (RPL10A)	RDTLYEAVRE	-	-	2.70
gi|15718687	40S ribosomal protein S3 (RPS3)	KLLGGLAVRR KDEILPTTPISEQKG KFVADGIFKA KAELNEFLTRE	- - - -	-	2.32 2.60 2.54 2.72
gi|89027564	60S ribosomal protein L6 (RPL6)	KFVIATSTKI KAVDSQILPKI	- -	-	2.39 2.44
gi|55961080	40S ribosomal protein S8 (RPS8)	RADGYVLEGKE KLTPEEEEILNKK KISSLLEEQFQQGKL	- - -	-	3.01 2.74 4.42
gi|16212066	S60S ribosomal protein L13 (RPL13)	KSTESLQANVQRL	-	-	3.39

		RTIGISVDPRR	-		2.51
7. Cell structure and motility					
gi|28336	β-tubilin	IIAPPER AGFAGDDAPR GYSFTTTAER AVFPSIVGRPR QEYDESGPSIVHR SYELPDGQVITIGNER VAPEEHPVLLTEAPLNPK	26 32 50 53 57 67 107	392	-
gi|19744388	Neuron navigator 2 (NAV2)	IALKGIAQR	34	34	-

a and b, the ion score and protein score were calculated respectively by MASCOT.
c, the score was calculated from Xcalibur software.

Supplement Table 2. The Proteins in the H2AX Complexes Derived from the Cells Irradiated by IR at 7.5 cGy and 10Gy Identified and Quantified by SILAC-based MS

NCBI accession no.	Protein name	Domain (SMART)	Domain (Pfam)	Fold of change[a]				No. of peptides
				7.5 cGy		10 Gy		
				ratio	S.D.[b]	ratio	S.D.	
1. Histones								
gi|48146275	Histone H2AX	H2A	Histone	-	-	-	-	5
gi|1568557	Histone H2B	H2B	Histone	0.99	0.03	0.98	0.02	3
gi|45767731	Histone H4	H4	Histone	0.80	0.11	0.75	0.06	7
2. DNA damage/repair response								
gi|13606056	PRKDC	PI3Kc	PI3_PI4_kinase, NUC194, FAT, FATC, HEAT	2.30	0.07	2.66	0.04	5
gi|49457432	Ku70	Ku78, SAP	Ku, Ku_C, Ku_N, SAP	2.78	0.61	2.84	0.69	3
gi|10863945	Ku86	Ku78, VWA	Ku, Ku_C, Ku_N, Ku_PK_bind	3.19	0.06	3.45	0.23	11
gi|37231	TOP2B	HATPase_c, TOP2c, Top4c	DNA_gyrase B, DNA_toposoIV, DTHCT, HATPase_c	1.36	0.15	1.15	0.10	4
3. Chromatin packaging and remodeling								
gi|6005757	SUPT16H		Peptidase_M24, Rtt106, SPT16	0.16	0.01	0.13	0.02	3
gi|189306	Nucleolin	RRM	FYDLN_acid, RRM_1	0.48	0.08	1.36	0.07	7
gi|825671	NPM1		Nucleoplasmin	0.41	0.01	0.10	0.01	5
gi|49457053	SET		NAP	0.18	0.01	0.11	0.02	3
gi|89040736	HMGN2	HMG17	HMG14_17	0.23	0.01	0.18	0.01	2
4. Cell cycle regulation								
gi|1155084	KIF11	KISc	Kinesin	0.51	0.03	0.83	0.10	10
gi|97537467	THRAP3			0.54	0.08	1.19	0.04	6
gi|11095436	VCP	AAA	AAA,	0.36	0.04	0.44	0.05	2

gi|7387554	BUB3	WD40	CDC48_2, CDC48_N WD40	0.16	0.01	0.05	0.01	2
5. p53 regulation								
gi|22902366	PARP1	WGR, BRCT	WGR, BRCT, PARP_reg, zf-PARP, PADR1, PARP	0.70	0.12	1.76	0.23	22
gi|47605556	BCLAF1			0.74	0.02	1.46	0.03	4
gi|31874030	RBM10	G_patch, RRM, ZnF_C2H2, ZnF_RBZ	G-patch, RRM_1, zf-RanBP	0.66	0.10	1.54	0.02	4
gi|38174276	p53BP3	RING	Zf-C3HC4	0.77	0.05	0.61	0.02	2
gi|56417899	HUWE1	HECTc, UBA	DUF908, DUF913, HECT, UBA, WWE	0.31	0.03	0.45	0.04	2

a, For each arginine-containing peptide, a set of three isotope signals spacing by 6 Da and 10 Da were observed as the 'light (L0)' isotope peak was originally from the non-irradiated cells, respectively. The ratio of any paired heavy *versus* light isotope signals, *i.e.*, H6/L0 or H10/L0, was then correlated with the IR-induced dose-dependent abundance of individual protein bound to H2AX (bait). For most of non-specific contaminants their H/L ratios were close to a unity because of their possibly equal distribution in each immunoprecipitate, *e.g.*, hnRNPA1 (Fig. 1b).

b, Standard deviation (S.D) was obtained from the average of the L/H ratio of each peptide derived from individual proteins. We found the relative standard deviation (RSD) for quantitative measurements of H/L ratio was at 8.9 % and then used 3-fold RSD which was approximately equal to 30% changes in the H2AX-bound abundances as the threshold. LDIR, low-dose ionizing radiation (7.5 cGy of IR). HDIR, high-dose ionizing radiation (10 Gy of IR).

Supplement Table 3. The Identified H2AX-interacting Proteins and the Domains They Contain Revealed by SMART and Pfam

Protein Name	**Domain Name** (SMART)	**Domain Name** (Pfam)
Histone H2AX	H2A	Histone
Histone H2B	H2B	Histone
Histone H4	H4	Histone
PRKDC	PI3Kc	PI3_PI4_kinase, NUC194, FAT, FATC, HEAT
Ku70	Ku78, SAP	Ku, Ku_C, Ku_N, SAP
Ku86	Ku78, VWA	Ku, Ku_C, Ku_N, Ku_PK_bind
TOP2B	HATPase_c, TOP2c, Top4c	DNA_gyraseB, DNA_toposoIV, DTHCT, HATPase_c
SUPT16H		Peptidase_M24, Rtt106, SPT16
Nucleolin	RRM	FYDLN_acid, RRM_1
NPM1		Nucleoplasmin
SET		NAP
HMGN2	HMG17	HMG14_17
KIF11	KISc	Kinesin
THRAP3		
VCP	AAA	AAA, CDC48_2, CDC48_N
BUB3	WD40	WD40
PARP1	WGR, BRCT	WGR, BRCT, PARP_reg, zf-PARP, PADR1, PARP
BCLAF1		
RBM10	G_patch, RRM, ZnF_C2H2, ZnF_RBZ	G-patch, RRM_1, zf-RanBP
p53BP3	RING	Zf-C3HC4
HUWE1	HECTc, UBA	DUF908, DUF913, HECT, UBA, WWE
Histone H1b	H15	Linker_histone
Histone H2AE	H2A	Histone
Histone H3	H3	Histone
Histone microH2A1.2	H2A	Histone
Calmodulin	EFh	efhand
TRPV3	ANK	Ank

		Ion_trans
Importin 9		IBN_N
HASPP28		PP28
RACK1	WD40	WD40
NUCKS		
MCM5	MCM	MCM
PRMT5		PRMT5
MEP50	WD40	WD40
Methylosome subunit pICln		ICln_channel
Proteasome 26S non-ATPase subunit 13 isoform 2	PINT	PCI
HSP90AA1	HATPase_c	HSP90, HATPase_c
Endoplasmin precursor (HSP90B1)	HATPase_c	HSP90, HATPase_c
HSPA5		HSP70
Heat shock 70 kDa protein 7 (HSPA7)		HSP70
UCHL5		Peptidase_C12
NIMA-related kinase 6	S_TKc	Pkinase
JHDM3A	JmjC, JmjN, PHD, TUDOR	JmjC, JmjN, PHD
WRN	35EXOc, DEXDc, HELICc, HRDC	3_5_exonuc, DEAD, Helicase_C, HRDC, RQC
PNKP		PNK3P
Topoisomerase I	TOPEUc	Topoisom_I_N, Topoisom_I
NUBP1	AAA	ParA
SMARCAL1	DEXDc, HELICc	HARP, Helicase_C, SNF2_N
SMRC1	CHROMO, SANT	Myb_DNA-binding, SWIRM
BPTF	BROMO,DDT,PHD	Bromodomain, DDT, FYDLN-acid, PHD
PABP1	PolyA, RRM	PABP, RRM_1
NOLC1	LisH	SRP40_C
HOXB1	HOX	Homebox
ZRANB3	HNHc	HNH
SMYD2	SET	Zf-MYND
HNRNPU	SAP, SPRY	SAP, SPRY

HNRNPA1	RRM	RRM_1
HNRNPCL1	RRM	RRM_1
SNRPB	Sm	LSM
EIF3I	WD40	WD40
EIF4B	RRM	RRM_1
RPL27A		L15
RPL13		Ribosomal_L13e
RPL10A		Ribosomal_L1
RPS3	KH	KH_2, Ribosomal_S3_C
RPL6		Ribosmal_L6e, Ribosomal_L6e_N
RPS8		Ribosmal_S8e
NAV2	AAA, CH	CH
GNB2L1	WD40	WD40

Supplement Table 4. Putative DNA-PKcs Target Sites for BCLAF1 Phosphorylation Predicted by GPS 2.1 Software with a High Threshold Setting

Position	Code	Peptide	Score[4]
15[1]	S	SHSSRSK**S**RSQSSSR	3.571
17	S	SSRSKSR**S**QSSSRSR	7.429
23	S	RSQSSSR**S**RSRSHSR	3.048
25	S	QSSSRSR**S**RSHSRKK	3
122[2]	S	PKRRSVS**S**QRSRSRS	4.381
144	S	RSPRSSS**S**RSSSPYS	3.286
151[3]	S	SRSSSPY**S**KSPVSKR	4.238
161	S	PVSKRRG**S**QEKQTKK	3.762
181	S	QEESPLK**S**KSQEEPK	3.619
183	S	ESPLKSK**S**QEEPKDT	6.048
237	S	SPIATPP**S**QSSSCSD	4.857
259	S	HSAKNTP**S**QHSHSIQ	7.19
494	T	RITVKKE**T**QSPEQVK	5.095
753	S	QDHSRSS**S**SSASPSS	3
760	S	SSSASPS**S**PSSREEK	2.952
763	S	ASPSSPS**S**REEKESK	5.857
769	S	SSREEKE**S**KKEREEE	3.714

1. the predicted phosphorylation sites in the RS domain are highlighted in grey,
2. the phosphorylation site in the basic zipper (bZIP) DNA binding domain is underlined,
3. the phosphorylation sites identified by mass spectrometry are highlighted in red,
4. the threshold of cut-off score is at 3.806 in the phosphorylation prediction by using GSP 2.1 software.